

FAST ACCRETION OF SMALL PLANETESIMALS BY PROTOPLANETARY CORES.

R. R. RAFIKOV

IAS, Einstein Dr., Princeton, NJ 08540

Draft version May 22, 2019

ABSTRACT

The dynamics of small planetesimals in the vicinity of protoplanetary cores immersed in a gaseous nebula is explored. Gas drag strongly affects the motion of small bodies leading to the decay of their eccentricities and inclinations, which are excited by the gravity of protoplanetary cores. Drag acting on larger ($\gtrsim 1$ km), high velocity planetesimals causes a mere reduction of their average random velocity. By contrast, drag qualitatively changes the dynamics of smaller ($\lesssim 1$ km), low velocity objects: (1) small planetesimals sediment towards the midplane of the nebula forming vertically thin subdisk; (2) their random velocities rapidly decay between successive passages of the cores and, as a result, encounters with cores typically occur at the minimum relative velocity allowed by the shear in the disk. This leads to a drastic increase in the accretion rate of small planetesimals by the protoplanetary cores, allowing cores to grow faster than expected in the simple oligarchic picture, provided that the population of small planetesimals contains more than roughly 1% of the solid mass in the nebula. Fragmentation of large planetesimals ($\gtrsim 1$ km) in energetic collisions triggered by the gravitational scattering by cores can easily channel this amount of material into small bodies on reasonable timescales (< 1 Myr in the outer Solar System), providing a means for the rapid growth (within several Myr at 30 AU) of 10^{26} g protoplanetary cores. Effects of inelastic collisions between planetesimals and presence of multiple protoplanetary cores are discussed.

Subject headings: planetary systems: formation — solar system: formation — Kuiper Belt

1. INTRODUCTION.

The formation of terrestrial planets and solid cores of giant planets is thought to proceed via the gravity-assisted merging of a large number of planetesimals — solid bodies with initial sizes of roughly several kilometers. Despite a considerable progress made in this field since the pioneering works of Safronov (1969), a number of important problems still remain unsolved. One of the most serious questions has to do with the time needed for planets to complete their growth to present sizes. In the framework of conventional theory this time is rather long, especially in the outer parts of the protoplanetary nebula ($\gtrsim 10^8 - 10^9$ yr), and it is likely that the gaseous component of the nebula dissipates much earlier (in $\lesssim 10^6 - 10^7$ yr). This would make it very hard for the giant planets in our Solar System to accrete their huge gaseous envelopes via core instability (Mizuno 1980) which is otherwise considered to be an attractive scenario.

Wetherill & Stewart (1989) have identified a very rapid “runaway” regime of accretion of protoplanetary cores which at the time seemed like a solution of this problem. However, later on Ida & Makino (1993) and Kokubo & Ida (1996, 1998) have demonstrated that the runaway accretion would persist only through a rather limited interval of time and that the final growth of protoplanetary cores to isolation (which corresponds to roughly 10^{26} g at 1 AU) would proceed in a slow manner, making the formation of cores of giant planets rather problematic.

These studies usually implied that the gaseous component of the nebula plays a secondary role in the planet formation process. Planetesimals were typically assumed to be rather massive ($10^{23} - 10^{24}$ g) bodies which are

only weakly affected by the gas (Kokubo & Ida 1998). This allows gravity to excite energetic random motions of planetesimal which decreases the role of gravitational focusing and reduces the efficiency of accretion. The purpose of this paper is to relax this assumption and to see what impact is produced on the planet formation picture by allowing most of the planetesimals to be small ($\lesssim 10$ km) bodies immersed in a gaseous environment. Such planetesimals would be appreciably affected by the gas drag and we will demonstrate that this can bring qualitative changes to their dynamics in the vicinity of the protoplanetary cores and, consequently, to the behavior of the mass accretion rate of cores.

Throughout this study we will use the following approximation to the structure of the Minimum Mass Solar Nebula (MMSN):

$$\Sigma_g(a) \approx 100 \Sigma_p \approx 3000 \text{ g cm}^{-2} a_{AU}^{-3/2}, \quad (1)$$

$$c_s(a) \approx 1.2 \text{ km s}^{-1} a_{AU}^{-1/4}, \quad (2)$$

where Σ_p, Σ_g are the solid and gas surface densities correspondingly, c_s is the gas sound speed, and $a_{AU} \equiv a/(1 \text{ AU})$ is a distance from the Sun a scaled by 1 AU. We will use the terms “protoplanetary core” and “protoplanetary embryo” interchangeably. Physical density of planetesimals ρ_p is always assumed to be 1 g cm^{-3} .

The paper is organized as follows: after a discussion of different gas drag regimes in §2 we proceed to the description of the planetesimal dynamics in the vicinity of protoplanetary cores in §3. The inclination of small planetesimals, a question very important for this study, is explored in §3.3.4. The separation of different gas drag and dynamical regimes in different parts of the nebula is described in §3.3.5 and lower limits on the random velocities of planetesimals are obtained in 4. The role of small planetesimals in the growth of protoplanetary

cores is studied in §6 and some important consequences for the planet formation picture are discussed in §7.

2. SUMMARY OF DIFFERENT GAS DRAG REGIMES.

Drag force acting on a body moving in a gaseous medium depends on the relative velocity of the body with respect to the gas v_r and on the ratio of its radius r_p to the molecular mean free path λ (Whipple 1972; Weidenschilling 1977). Whenever $r_p \lesssim \lambda$ the Epstein drag law applies:

$$\frac{d\mathbf{v}_r}{dt} \simeq -\frac{\rho_g c_s}{\rho_p r_p} \mathbf{v}_r = -\Omega \frac{\Sigma_g}{\rho_p r_p} \mathbf{v}_r, \quad (3)$$

where Ω is the angular frequency of the disk, ρ_g is the gas density, r_p is the planetesimal size, and ρ_p is the physical density of planetesimals (planetesimal random velocities are assumed to be subsonic). For an adopted MMSN model (2) we estimate the molecular mean free path to be

$$\lambda = (n_g \sigma_{H_2})^{-1} = \frac{\mu c_s}{\Omega \Sigma_g \sigma_{H_2}} \simeq 1 \text{ cm } a_{AU}^{11/4} \quad (4)$$

for H_2 collision cross section $\sigma_{H_2} \simeq 10^{-15} \text{ cm}^2$ (μ is the mean molecular weight). It is important to notice that λ increases very rapidly with the distance from the Sun, so that although only sub-cm particles can experience Epstein drag at 1 AU, at 30 AU this drag regime is valid even for rocks 100 m in size!

A large spherical body with $r_p \gtrsim \lambda$ experiences the deceleration in the following form:

$$\frac{d\mathbf{v}_r}{dt} \simeq -C_D \frac{3}{4\pi} \frac{\rho_g}{\rho_p r_p} v_r \mathbf{v}_r. \quad (5)$$

Drag coefficient C_D is a function of the Reynolds number $Re \equiv r_p v_r / \nu$, where ν is a kinematic viscosity. We assume that there is only molecular viscosity, i.e. $\nu \simeq \lambda c_s / 3$; in the presence of anomalous sources of viscosity the expression for ν has to be correspondingly adjusted.

For $Re \lesssim 1$ gas drag is in the Stokes regime (Landau & Lifshitz 1987), meaning that $C_D = 6\pi Re^{-1}$. For $Re \gg 1$ drag coefficient becomes constant: $C_D \simeq 0.7$ (Weidenschilling 1977). We neglect the more complicated behavior of C_D for $1 \lesssim Re \lesssim 10^2$ (Whipple 1972) and simply assume that C_D switches from one asymptotic behavior to the other at $Re_b \simeq 20$. Thus, we adopt

$$\frac{d\mathbf{v}_r}{dt} \simeq -\frac{3}{2} \Omega \frac{\Sigma_g}{\rho_p r_p} \frac{\lambda}{r_p} \mathbf{v}_r, \quad Re \lesssim Re_b, \quad (6)$$

$$\frac{d\mathbf{v}_r}{dt} \simeq -0.2 \Omega \frac{\Sigma_g}{\rho_p r_p} \frac{v_r}{c_s} \mathbf{v}_r, \quad Re \gtrsim Re_b. \quad (7)$$

Gas drag acting on a planetesimal moving on an elliptic and inclined orbit leads to the decay of planetesimal eccentricity e , inclination i , and semimajor axis a (Adachi et al. 1976). Square of the random component of the planetesimals velocity v^2 is a weighted sum of $(e\Omega a)^2$, $(i\Omega a)^2$. We approximate this relationship by the asymptotically valid expression $v \approx \Omega a(e + i)$ omitting any constant factors. For the calculation of the decay rate of the orbital elements it is important to take into account the sub-Keplerian angular velocity of the gas in the nebula caused by the radial pressure support. This

gives rise to the additional azimuthal contribution Δv_g to the relative gas-planetesimal velocity. One can easily demonstrate that

$$\Delta v_g \approx \Omega a \left(\frac{c_s}{\Omega a} \right)^2 \equiv \Omega a \eta \simeq 50 \text{ m s}^{-1}, \quad (8)$$

$$\eta \equiv \left(\frac{c_s}{\Omega a} \right)^2 \simeq 1.6 \times 10^{-3} a_{AU}^{1/2}. \quad (9)$$

For our adopted temperature profile Δv_g is independent of a . Whenever random velocity of planetesimal exceeds Δv_g this velocity offset provides only a small contribution to the relative gas-planetesimal velocity. In the opposite case the relative velocity is dominated by Δv_g .

Using (3)-(7) we can introduce a *damping time* t_d — typical time needed to decelerate planetesimals by the gas drag if their initial velocity with respect to the gas is Δv_g . Using equations (3), (6), & (7) one obtains

$$t_d \approx 5 \Omega^{-1} \frac{\rho_p r_p}{\Sigma_g} \frac{\Omega a}{c_s}, \quad (10)$$

$$t_d \approx \frac{2}{3} \Omega^{-1} \frac{\rho_p r_p}{\Sigma_g} \frac{r_p}{\lambda}, \quad (11)$$

$$t_d \approx \Omega^{-1} \frac{\rho_p r_p}{\Sigma_g} \quad (12)$$

for the quadratic, Stokes, and Epstein drag regimes respectively.

When $t_d \ll \Omega^{-1}$ planetesimal motion is tightly coupled to that of the gas; critical planetesimal size r_{stop} at which the transition from almost Keplerian motion to the sub-Keplerian gas rotation occurs can be determined from the condition $t_d \approx \Omega^{-1}$. Using (10)-(12) we find that

$$r_{stop} \approx 0.2 \frac{\Sigma_g}{\rho_p} \frac{c_s}{\Omega a} \approx 20 \text{ cm } a_{AU}^{-5/4}, \quad (13)$$

$$r_{stop} \approx \left(\frac{3}{2} \frac{\Sigma_g}{\rho_p} \lambda \right)^{1/2} \approx 70 \text{ cm } a_{AU}^{5/8}, \quad (14)$$

$$r_{stop} \approx \frac{\Sigma_g}{\rho_p} \approx 3 \times 10^3 \text{ cm } a_{AU}^{-3/2}, \quad (15)$$

for the quadratic, Stokes, and Epstein drag regimes.

Calculation of the orbital evolution of planetesimals bigger than r_{stop} due to the gas drag was performed by Adachi et al. (1976; see also Tanaka & Ida 1997) taking into account the saturation of the relative gas-planetesimal velocity when the planetesimal random speed is $\lesssim \Delta v_g$. We quote their results for different drag regimes keeping only the most important contributions¹:

$$\frac{1}{e^2} \frac{de^2}{dt} \approx \frac{2}{i^2} \frac{di^2}{dt} \approx -0.2 \Omega \frac{\Sigma_g}{\rho_p r_p} \frac{\Omega a}{c_s} (e + i + \eta), \quad (16)$$

$$\frac{1}{a} \frac{da}{dt} \approx -0.2 \Omega \frac{\Sigma_g}{\rho_p r_p} \frac{\Omega a}{c_s} \eta (e + i + \eta), \quad (17)$$

for the quadratic dependence (7) of gas drag on velocity. The decay rates represented by equations (16) & (17) behave differently for $e, i \lesssim \eta$ and $e, i \gtrsim \eta$. In the first case the relative gas-planetesimal velocity is close to Δv_g ; as a result, orbital elements exponentially decay with time.

¹ We have set to unity all numerical factors which appear in the course of orbital averaging; however we kept initial factors since some of them (e.g. in [7]) are significantly different from unity.

In the second case v_r is dominated by the planetesimal random motion and the decay time is inversely proportional to the random velocity v .

For the linear dependence of drag on v_r represented by the equations (3) and (6) one finds (Adachi et al. 1976)

$$\frac{1}{e^2} \frac{de^2}{dt} \approx \frac{2}{i^2} \frac{di^2}{dt} \approx -\Omega \zeta \frac{\Sigma_g}{\rho_p r_p}, \quad (18)$$

$$\frac{1}{a} \frac{da}{dt} \approx -\Omega \zeta \frac{\Sigma_g}{\rho_p r_p} \eta, \quad (19)$$

where $\zeta = 1$ for $r_p \lesssim \lambda$ (Epstein drag [3]), and $\zeta = (3/2)\lambda/r_p$ for $r_p \gtrsim \lambda$, $Re \lesssim Re_b$ (Stokes drag [6]).

3. SCATTERING BY THE MASSIVE PROTOPLANETARY CORES.

Let us consider the scattering of a planetesimal by a single protoplanetary core moving on a circular and uninclined orbit. The velocity perturbation which planetesimal receives in the course of gravitational interaction depends on the separation of the planetesimal guiding center from the embryo's orbit and on the planetesimal approach velocity v_a .

It is well known (Hénon & Petit 1986) that the Hill radius R_H of interacting bodies sets an important length scale for the scattering in the disk. For two bodies with masses m_1 and m_2 Hill radius is defined as

$$R_H \equiv a \left(\frac{m_1 + m_2}{M_\odot} \right)^{1/3}. \quad (20)$$

In the case of scattering of planetesimals by a massive protoplanetary embryo with mass M_e Hill radius is determined solely by M_e : $R_H = a(M_e/M_\odot)^{1/3}$.

For our purposes the planetesimal approach velocity can be represented as $v_a \approx \Omega(ea + ia + R_H)$ and it is different from the horizontal random velocity $v_h \equiv e\Omega a$ and vertical random velocity $v_z \equiv i\Omega a$. Additional contribution to v_a in the form of the shear across the Hill radius ΩR_H (sometimes called the Hill velocity) appears because of the differential rotation of the disk. Gravitational focusing of the planetesimals by the embryo is determined by v_a . Velocity v_z determines the vertical thickness of planetesimal disk, thus it regulates the volume number density of planetesimals n_p for a given surface mass density Σ_p : $n_p = \Omega \Sigma_p / (v_z m_p)$, where $m_p \equiv (4\pi/3)\rho_p r_p^3$ is a planetesimal mass. Vertical velocity is much smaller than v_a or the total random velocity $v \approx v_h + v_z$ when $i \ll e$.

Whenever random velocity v is less than ΩR_H — the so-called *shear-dominated* regime — close approaches between the gravitationally interacting bodies which might lead to their physical collision are only possible for the orbital separation h less than $\sim R_H$. For $h \gg R_H$ (distant encounters) orbital perturbations incurred in the course of scattering are small: changes of the random velocity Δv and of the orbital separation Δh produced by *single* scattering have magnitudes

$$\Delta v \approx \Omega R_H (R_H/h)^2, \quad \Delta h \approx R_H (R_H/h)^2. \quad (21)$$

These increments can be positive or negative depending on the orbital phases of bodies and their random velocities before the encounter. The averages of these quantities over epicyclic phases were calculated by Hasegawa &

Nakazawa (1990) and we quote here their result for the eccentricity (it will be used in §4):

$$\langle \Delta(e^2) \rangle \approx 5 (R_H/a)^2 \left(\frac{R_H}{h} \right)^4. \quad (22)$$

In the case $h \sim R_H$, when interacting bodies enter their mutual Hill sphere, strong scattering takes place:

$$\Delta v \approx \Omega R_H, \quad \Delta h \approx R_H, \quad (23)$$

with both increments being positive — orbits are repelled and random velocity of the order of ΩR_H is excited. At the same time, from purely geometrical considerations it is clear that the change of vertical velocity is proportional to the vertical projection of the random velocity perturbation, and is much smaller than the change in horizontal velocity:

$$\Delta v_z \sim \Delta v \frac{v_z}{v_a} \approx v_z, \quad \text{or} \quad \Delta i \sim i. \quad (24)$$

Since total velocity increment Δv is of the order or bigger than the initial random velocity of planetesimals, scattering for $h \sim R_H$ in the shear-dominated regime has a *discrete* character.

Another possible dynamical state is the *dispersion-dominated* regime which takes place whenever $v \gtrsim \Omega R_H$. In this case the epicyclic excursions of planetesimals allow collisions between bodies with orbits separated by $h < v/\Omega$; more distant bodies are again subject to only weak scattering. Moreover, even particles having close approaches experience *on average* only small velocity perturbation compared to the pre-encounter velocity v_a . This allows one to treat the scattering in the dispersion-dominated regime as a *continuous* process. Another important feature of the dispersion-dominated regime is that $v_z \sim v_h$, or $i \sim e$, as a result of roughly three-dimensional nature of scattering in this regime which tends to isotropize highly anisotropic velocity distributions. Thus, it is enough to follow the evolution of only one component of planetesimal velocity (e.g. e) in the dispersion-dominated regime.

3.1. Quadratic drag.

Let's now proceed to consider planetesimal dynamics for different gas drag regimes. First, we explore the case of quadratic drag represented by equations (7) and (16), (17) which is valid for $r_p \gtrsim \lambda$, $Re \gtrsim Re_b$. This situation would most likely be realized in the inner parts of the protoplanetary nebula since λ is rather small there making Epstein regime irrelevant and bringing Reynolds number to a high value.

Let's first assume that scattering occurs in the dispersion-dominated regime and try to figure out under which conditions a steady state can be realized in this case. Gravitational scattering by the embryo increases planetesimal random energy at a rate² (Ida & Makino 1993; Rafikov 2003b)

$$\frac{dv^2}{dt} \approx \Omega (\Omega R_H)^2 \frac{R_H}{a} \left(\frac{\Omega R_H}{v} \right)^3 \ln \Lambda, \quad (25)$$

where $\ln \Lambda \sim 1$ is a Coulomb logarithm which for $e \sim i \gtrsim R_H/a$ can be estimated as $\Lambda \approx (v/\Omega R_H)^3$ (Stewart

² In dispersion-dominated regime $v_a \approx v$.

& Ida 2000). Because of the very weak dependence of the Coulomb logarithm on velocity we will set it to unity in our further discussion.

Balancing this growth rate by the damping due to the gas drag represented by equation (16) we find that

$$\begin{aligned} v &\approx \Omega R_H \left(5 \frac{c_s}{\Omega a} \frac{\rho_p r_p}{\Sigma_g} \right)^{1/6} \\ &\approx 2 \Omega R_H \left(\frac{r_p}{10 \text{ km}} \right)^{1/6} a_{AU}^{7/24}, \quad v \gtrsim \Delta v_g, \quad (26) \\ v &\approx \Omega R_H \left(5 \frac{c_s}{\Omega a} \frac{\rho_p r_p}{\Sigma_g} \frac{R_H}{\eta a} \right)^{1/5} \\ &\approx 2.4 \Omega R_H \left(\frac{r_p}{10 \text{ km}} \right)^{1/5} \left(\frac{M_e}{10^{25} \text{ g}} \right)^{1/15} a_{AU}^{1/4}, \\ &\quad v \lesssim \Delta v_g. \quad (27) \end{aligned}$$

For further convenience we normalize the embryo's mass M_e to a fiducial mass M_f and planetesimal radius to a fiducial radius r_f which are defined as

$$M_f \equiv M_\odot \eta^3 \simeq 8 \times 10^{24} \text{ g } a_{AU}^{3/2}, \quad (28)$$

$$r_f \equiv 0.2 \frac{\Sigma_g}{\rho_p} \frac{\Omega a}{c_s} = 0.2 a \frac{\rho_g}{\rho_p} \simeq 150 \text{ m } a_{AU}^{-7/4}. \quad (29)$$

These two parameters uniquely characterize the dynamics of the embryo-planetesimal scattering when the gas drag dependence on the velocity is represented by equation (7). Using this notation we conclude from (26) that $v \gtrsim \Omega R_H$ and $v \gtrsim \Delta v_g$ if

$$r_p/r_f \gtrsim 1, \quad (30)$$

$$M_e/M_f \gtrsim (r_p/r_f)^{-1/2}. \quad (31)$$

From (27) we find that $v \gtrsim \Omega R_H$ and $v \lesssim \Delta v_g$ if

$$M_e/M_f \gtrsim (r_p/r_f)^{-3}, \quad (32)$$

$$M_e/M_f \lesssim (r_p/r_f)^{-1/2}. \quad (33)$$

Thus, conditions (30) and (32) determine the region in the parameter space $M_e - r_p$ in which planetesimals are dispersion-dominated with respect to the embryo and maintain a steady-state velocity dispersion.

Whenever both (30) and (32) are not fulfilled the scattering of planetesimals proceeds in the shear-dominated regime. As we mentioned previously, this type of interaction has a discrete nature — gas drag causes significant evolution of planetesimal velocity between close approaches to the embryo. We consider a planetesimal initially separated from the embryo by $h \sim R_H$ in semi-major axis with initial random velocity $v \lesssim \Omega R_H$. Immediately after scattering v increases to $\sim \Omega R_H$. Note that when $M_e \gtrsim M_f$ random velocity right after encounter is higher than Δv_g and its damping by the gas drag is very efficient: $dv^2/dt \propto -v^3$, see equation (7). In the opposite case $M_e \lesssim M_f$ planetesimal velocities never exceed Δv_g in the shear-dominated regime; as a result, v damps exponentially.

We will see in §3.4 that the inclination of planetesimals interacting with the embryo in the shear-dominated regime is typically much smaller than their eccentricity. Then we can easily solve equation (7) to obtain a general solution in the form

$$e(t) \approx \eta \left[(1 + \eta/e_0) \exp \left(\Omega t \eta \frac{r_f}{r_p} \right) - 1 \right]^{-1}, \quad (34)$$

where $e_0 \sim R_H/a = \eta(M_e/M_f)^{1/3}$ is the eccentricity of planetesimal right after its encounter with the embryo and t is the time since the last scattering took place.

For low-mass embryos, $M_e \lesssim M_f$, post-encounter eccentricity e_0 is smaller than η , and (34) reduces to exponential damping:

$$e(t) \approx e_0 \exp \left(-\Omega t \eta \frac{r_f}{r_p} \right) \approx \eta \left(\frac{M_e}{M_f} \right)^{1/3} e^{-t/t_d}. \quad (35)$$

Thus, eccentricity decays on a typical timescale t_d , see (10).

For high-mass embryos, $M_e \gtrsim M_f$, post-encounter velocity is above Δv_g and we find that

$$e(t) \approx \frac{\eta}{(\eta/e_0) + \Omega t \eta (r_f/r_p)} = \frac{\eta}{(\eta/e_0) + (t/t_d)}, \quad (36)$$

for $t \lesssim t_d$. One finds that $e \approx \eta$ at $t \approx t_d$ independent of the initial post-encounter eccentricity. Beyond that point relative gas-planetesimal velocity is determined by Δv_g , thus for $t \gtrsim t_d$ eccentricity decays exponentially on a timescale t_d , analogous to (35). It also follows from (36) that significant reduction of eccentricity after scattering by high mass embryo occurs already on a timescale $t_d(\eta/e_0) \approx \Omega^{-1}(r_p/r_f)(a/R_H) \ll t_d$.

Planetesimals separated from the embryo in semi-major axis by $\sim R_H$ pass the embryo's Hill sphere (and experience strong scattering) roughly every synodic period t_{syn} for $1R_H$ radial separation:

$$t_{syn} \approx \Omega^{-1}(a/R_H). \quad (37)$$

Requiring the damping time t_d to be shorter than t_{syn} (which is necessary for the shear-dominated regime to hold) for embryos less massive than M_f is equivalent to demanding that

$$\eta^{-1}(r_p/r_f) \lesssim a/R_H \quad \text{or} \quad M_e/M_f \lesssim (r_p/r_f)^{-3}. \quad (38)$$

For embryos with $M_e \gtrsim M_f$ eccentricity is strongly damped below its initial value between the consecutive encounters with the embryo if $t_d(\eta/e_0) \lesssim t_{syn}$ or if

$$(r_p/r_f)(a/R_H) \lesssim a/R_H \quad \text{or} \quad r_p/r_f \lesssim 1. \quad (39)$$

At the same time, the eccentricity would not drop below η before the next encounter occurs if (38) is not fulfilled simultaneously with (39).

Comparing (38) and (39) with the dispersion-dominated conditions (30) and (32) we see that depending on M_e/M_f and r_p/r_f there can only be two possible states in the system: either planetesimals are scattered in a smooth, continuous fashion in the dispersion-dominated regime, with gas drag not capable of damping their eccentricities significantly between the consecutive approaches to the embryo, or they are strongly scattered by the embryo at each approach and gas appreciably reduces their random velocities before the next encounter takes place.

The discrete nature of planetesimal scattering by the embryo in the shear-dominated regime is very important for determining the approach velocity of planetesimal to the embryo. For example, if we were to assume that scattering in the shear-dominated regime is continuous (like in the dispersion-dominated case) the average rate of eccentricity growth would have the form $de/dt \sim (R_H/a)/t_{syn}$, since embryo increases planetesimal eccentricity by $\sim R_H/a$ every synodic period. Balancing this

by the gas drag in the form (7), one would find the average value of eccentricity to be $\sim (R_H/a)(t_d/t_{syn})$. It would however be a grave mistake to assume that this is the eccentricity with which planetesimal approaches the embryo. Indeed, it follows from (35) that the planetesimal eccentricity right before the next encounter with the embryo is $\sim (R_H/a) \exp(-t_{syn}/t_d)$ for $M_e \lesssim M_f$, which is exponentially smaller than the average value of eccentricity! Thus, the proper treatment of the shear-dominated regime taking the discrete nature of scattering into account is very important for figuring out the initial conditions of the interaction process. This will have important ramifications for the question of accretion of these planetesimals as we demonstrate in §6.

3.2. Stokes drag.

Planetesimals interact with the gas in the Stokes regime when $r_p \gtrsim \lambda$ and $Re \lesssim Re_b$. The last condition depends not only on the particle size r_p but also on its velocity. An important velocity in this problem is Δv_g : if planetesimal interacts with the embryo in the shear-dominated regime and $M_e \lesssim M_f$, planetesimal velocity never exceeds Δv_g . Thus, we can introduce another fiducial size, r_S , which we define as the planetesimal size for which $Re = Re_b$ at $v = \Delta v_g$:

$$r_S \equiv \lambda \frac{Re_b}{3} \frac{\Omega a}{c_s} \approx 2 \text{ m } a_{AU}^{5/2}. \quad (40)$$

Embryos more massive than M_f endow shear-dominated planetesimals with velocity $\Omega R_H > \Delta v_g$ at each scattering episode. But even then planetesimals with sizes satisfying

$$M_e/M_f \lesssim (r_p/r_S)^{-3} = \left(\frac{r_S}{r_f}\right)^3 (r_p/r_f)^{-3} \quad (41)$$

experience *only* the Stokes drag, i.e. their maximum velocity and physical size are never large enough for their Reynolds number to exceed Re_b . Planetesimals scattered by the more massive embryos would experience quadratic drag right after encounter (even if only temporarily) before switching to the Stokes regime. From equation (18) one can easily see that the damping between encounters is purely exponential for the Stokes drag independent of the planetesimal random velocity (similar to the quadratic drag for $e \lesssim \eta$, see §3.3.1).

Let us now turn to the dispersion-dominated regime. Balancing scattering rate (25) by the damping rate (18) with $\zeta = (3/2)\lambda/r_p$ we find that

$$v \approx \Omega R_H \left[\frac{2}{3} \left(\frac{M_e}{M_f}\right)^{1/3} \left(\frac{r_p}{r_f}\right)^2 \frac{r_f}{r_S} \right]^{1/5} \\ \approx 5 \Omega R_H \left(\frac{r_p}{1 \text{ km}}\right)^{2/5} \left(\frac{M_e}{10^{25} \text{ g}}\right)^{1/15} a_{AU}^{-1/4}. \quad (42)$$

Consequently, planetesimal is in the dispersion-dominated regime with respect to the embryo when

$$M_e/M_f \gtrsim \left(\frac{r_S}{r_f}\right)^3 (r_p/r_f)^{-6}. \quad (43)$$

Smaller planetesimals are in the shear-dominated regime and experience discrete scattering by the embryos.

From equation (42) we also find that $v \lesssim \Delta v_g$ whenever

$$M_e/M_f \lesssim \left(\frac{r_S}{r_f}\right)^{1/2} (r_p/r_f)^{-1}, \quad (44)$$

and that $Re < Re_b$ (and drag is in the Stokes regime) if

$$M_e/M_f \lesssim \left(\frac{r_S}{r_f}\right)^3 (r_p/r_f)^{-7/2}. \quad (45)$$

The last equation is a dispersion-dominated analog of the condition (41).

3.3. Epstein drag.

Smallest planetesimals, having physical sizes $\lesssim \lambda$, are coupled to the gas via the Epstein drag. Performing analysis analogous to that of §3.2 one finds that in the dispersion-dominated regime scattering by the embryo maintains planetesimal random velocity at the level of

$$v \approx \Omega R_H \left[\left(\frac{M_e}{M_f}\right)^{1/3} \frac{\lambda}{r_S} \frac{r_p}{r_f} \right]^{1/5} \\ \approx 1.4 \Omega R_H \left(\frac{r_p}{1 \text{ km}}\right)^{1/5} \left(\frac{M_e}{10^{25} \text{ g}}\right)^{1/15} \left(\frac{a_{AU}}{30}\right)^{3/10} \quad (46)$$

It follows from this formula that planetesimal can only be in the dispersion-dominated regime with respect to the embryo if

$$M_e/M_f \gtrsim \left(\frac{r_S}{\lambda}\right)^3 (r_p/r_f)^{-3}. \quad (47)$$

In this dynamical regime planetesimal velocity is below Δv_g only when

$$M_e/M_f \lesssim \left(\frac{r_S}{\lambda}\right)^{1/2} (r_p/r_f)^{-1/2}. \quad (48)$$

Planetesimals too small to satisfy (47) are in the shear-dominated regime and experience strong scattering by the embryo every synodic period, with their orbital elements exponentially decaying between encounters (analogous to the behavior in the case of Stokes drag, see §3.3.2).

3.4. Inclination evolution.

It is easy to see from equations (16) and (18) that as long as the gas drag is the only force affecting planetesimal after its encounter with the embryo, its inclination decays according to

$$i(t) \approx i_0 \sqrt{e(t)/e_0}, \quad (49)$$

where e_0, i_0 are the post-encounter values of eccentricity and inclination and $e(t)$ is given by (34) for quadratic gas drag. In the shear-dominated regime it might seem that $i \gg e$ long after the encounter took place (when $e \ll e_0$). This argument, however, assumes that $i_0 \sim e_0$ and we now show that this is not the case.

Indeed even if the initial inclination is of the order of R_H/a , it will be exponentially small right before the next encounter (see [35] and [49]) since the damping time is shorter than the synodic period in the shear-dominated regime. After this second encounter, according to (24), the inclination would not go back to R_H/a but would

remain small. Subsequent gas drag before the next passage of the embryo would reduce planetesimal inclination even more, and so on. As a result, we arrive at the very interesting conclusion: as long as planetesimal is in the shear-dominated regime its inclination keeps decaying. Thus, all shear-dominated planetesimals “rain out” towards the disk midplane and collapse into vertically thin layer. This emphasizes the importance of determining which part of the planetesimal population is shear-dominated with respect to the embryo.

If embryo is on purely uninclined orbit and the gas drag is the only process affecting planetesimal dynamics between encounters, the thickness of the layer would be zero. In reality, there are additional stirring agents which would keep the thickness of this subdisk finite, although still very small, and we consider them in §4 & §5.

3.5. Separation of different regimes.

We now summarize what we have learned in §3.3.1-3.3.3 about the planetesimal dynamics in different locations in the proto-Solar nebula.

First of all, from our previous discussion it is clear that the separation of different gas drag regimes sensitively depends on the relative values of the fiducial planetesimal sizes λ , r_f , and r_s given by the equations (4), (29), and (40). In Figure 1 we display the scaling of these sizes with the distance from the Sun. The boundary between the quadratic and Stokes drag regimes is calculated assuming $v \approx \Delta v_g$ and coincides with r_s . We also display the curve $r_{stop}(a)$ using equations (13)-(15) — planetesimals with r_p below this curve (shaded region) are tightly coupled to the gas and their dynamics cannot be described by equations (16)-(19).

From Figure 1 one can see that depending on the location in the nebula there could be three possible situations: (a) when $\lambda \lesssim r_s \lesssim r_f$, which holds for $a \lesssim 3$ AU in the MMSN, (b) when $\lambda \lesssim r_f \lesssim r_s$, which takes place for $3 \text{ AU} \lesssim a \lesssim 9 \text{ AU}$, and (c) when $r_f \lesssim \lambda \lesssim r_s$, which is valid for $a \gtrsim 9 \text{ AU}$.

The first case pertains to the region of terrestrial planets. We display possible regimes of planetesimal interaction with the gas in Figure 2. They are classified according to the values of planetesimal size r_p and embryo mass M_e . Thick solid line separates planetesimals which interact with the embryo in the shear-dominated regime and experience discrete scattering (hatched region to the left of the curve) from those which undergo the dispersion-dominated scattering (unhatched region). In the terrestrial region, as we see from Figure 2, this curve is set by equations (30) and (32). Dashed curves denote the boundaries of different gas drag regimes: Epstein drag is valid whenever $r_p \lesssim \lambda$; Stokes drag operates whenever $Re \lesssim Re_b$ — in the shear-dominated regime this means $r_p \lesssim r_s$ for embryos that cannot kick planetesimals by more than Δv_g ($M_e \lesssim M_f$, see §3.3.2), and restriction (41) for embryos that can³ ($M_e \gtrsim M_f$). For even bigger planetesimals the gas drag is quadratic and planetesimals can be either in the shear- (small ones) or in the

³ In fact, even near embryos more massive than M_e determined from (41) planetesimals can spend some time in the Stokes regime: although they are in the quadratic drag regime right after the passage of the embryo, their velocity rapidly decreases after that and their Reynolds number can drop below Re_b before the next encounter takes place.

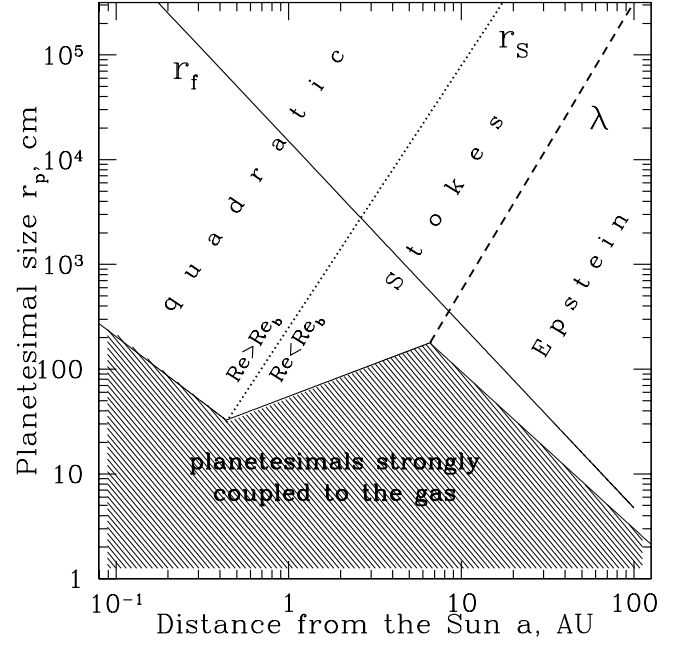


FIG. 1.— Behavior of the length scales r_f , r_s , and λ important for the planetesimal interaction with the gas (with different regimes marked on the plot), as functions of distance a from the Sun. Planetesimals with sizes in the shaded region have stopping time shorter than local Ω^{-1} and are thus moving together with the gas. Complex shape of the boundary of this region is due to the different gas drag regimes.

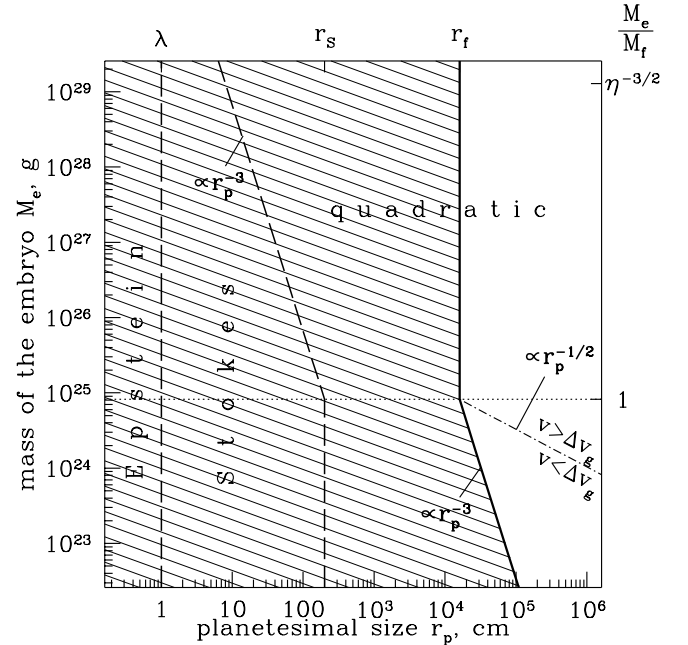


FIG. 2.— Separation of planetesimals into the shear- and dispersion-dominated ones with respect to the embryo in the phase space of the embryo’s mass M_e and planetesimals size r_p . This particular separation and numerical values indicated in the Figure pertain for the case $a = 1 \text{ AU}$ (terrestrial planet region), where $\lambda \lesssim r_s \lesssim r_f$. Thick solid line separates two dynamical regimes, with shear-dominated one being hatched. Thick dashed curves separate different regimes of planetesimal interaction with the gas (explicitly indicated on the plot). See text for more details.

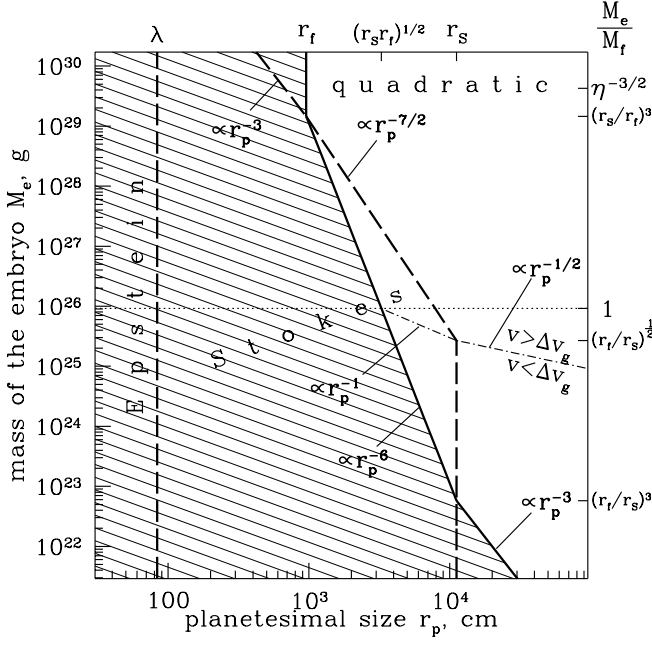


FIG. 3.— Same as Figure 2 but for the case $a = 5$ AU (giant planet region), where $\lambda \lesssim r_f \lesssim r_s$.

dispersion-dominated (large ones) regime. In the latter regime the dot-dashed line separates cases of equilibrium planetesimal random velocity being higher or lower than Δv_g , see equations (31) and (33). When considering the population of small planetesimals we should always keep in mind that our discussion in §3.3.1-3.3.2 is valid only for planetesimals moving on almost Keplerian orbits. Thus, a condition $r_p \gtrsim r_{stop}$ must be satisfied which restricts the validity of our results to planetesimals bigger than ~ 1 m (see Figure 1). Smaller planetesimals largely follow the motion of the gas. Embryo's mass is not allowed to exceed $\eta^{-3/2} M_f$ because more massive protoplanetary cores excite supersonic random velocities of surrounding planetesimals.

As we demonstrated in §3.4 in the shear-dominated regime small planetesimals sediment into the geometrically thin subdisk (thinner than the embryo's Hill radius) near the midplane of the nebula. We can readily see from the Figure 2 that in the terrestrial region this destiny awaits all planetesimals smaller than $\sim 100 - 200$ m in size (less than $\sim 10^{13} - 10^{14}$ in mass) in the vicinity of embryos more massive than about 10^{25} g. Near less massive embryos even larger planetesimals can belong to this dynamically cold population: only bodies bigger than about 1 km can escape this fate near 10^{23} g mass embryo. Thus, gas drag can have important effect even on kilometer size planetesimals when the question of their interaction with massive embryos is concerned.

Figure 3 represents the separation of different gas drag and dynamical regimes at 5 AU from the Sun ($\lambda \lesssim r_f \lesssim r_s$), corresponding to the giant planet region (roughly the semimajor axis of Jupiter). Evidently, the structure of the $M_e - r_p$ phase space is more complex in this part of the nebula. For example, planetesimals interacting with the embryo in the dispersion-dominated regime can now experience not only quadratic but also the Stokes

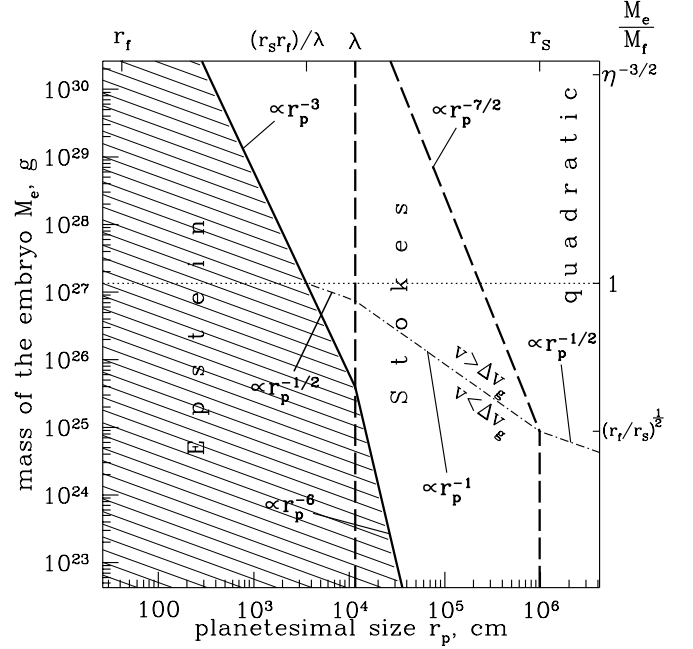


FIG. 4.— Same as Figure 2 but for the case $a = 30$ AU (region of ice giants), where $r_f \lesssim \lambda \lesssim r_s$.

drag. The reason for this is the lower Hill velocity ΩR_H for a given M_e at 5 AU which reduces the efficiency of planetesimal stirring by the embryo (see [25]) and diminishes the equilibrium planetesimal velocity. As a result, Reynolds number can drop below Re_b even in the dispersion-dominated regime and drag can switch to the Stokes regime for some bodies. Again, one should keep in mind that planetesimal smaller than about 1 m are tightly coupled to the gas at 5 AU, see Figure 1.

Boundaries of different drag regimes are computed using equations (41) and (45). Hatched region again represents M_e and r_p for which planetesimal scattering by the embryo occurs in the shear-dominated regime (its boundary is determined by equations [30], [32], and [43]). One can see that to be in this regime planetesimals have to be somewhat smaller than was necessary at 1 AU: $r_p \lesssim 30$ m for $M_e \approx 10^{26}$ g and $r_p \lesssim 100$ m for $M_e \approx 10^{23}$ g. This happens because gas density rapidly drops with the distance from the Sun and this tendency cannot be counteracted by longer synodic period at 5 AU (for a given M_e). Thus, somewhat less planetesimal material will be concentrated in the vertically thin subdisk of small bodies at 5 AU than at 1 AU, but the difference is not very large.

Finally, Figure 4 displays the situation at 30 AU (roughly the semimajor axis of Neptune), in the region of ice giants. Calculation of boundaries of different gas drag and dynamical regimes was performed using equations (33), (43)-(45), (47). From the Figure 1 we can easily see that the molecular mean free path λ is very large in this part of the nebula making the Epstein gas drag important in setting the boundary between the shear- and dispersion-dominated dynamical regimes. In this distant part of the nebula only bodies smaller than ~ 10 cm would be moving with the gas; for bigger bodies our results apply directly. For embryos with masses $10^{23} - 10^{27}$

g the critical planetesimal size below which scattering is shear-dominated is 50 – 300 m. The critical size is larger than at 5 AU because the gas drag in the Epstein and Stokes regimes is more efficient than in the quadratic regime (for the same r_p and M_e).

3.6. Migration, gaps, and multiple embryos.

The conservation of Jacobi constant ensures that any change in the energy of planetesimal random motion in the course of scattering by the embryo is accompanied by the change in planetesimal semimajor axis. As a result, planetesimal surface density distribution would be perturbed by the embryo and a gap might form (Ida & Makino 1993). For the shear-dominated planetesimals gap opening can be especially important, because in this dynamical regime planetesimal guiding centers are moved away from the embryo’s orbit by $\sim R_H$ in a single passage at $h \approx R_H$, see (23) (Rafikov 2001). If this happens, accretion of planetesimals by the embryo can be severely affected (Rafikov 2003a).

At the same time, gas drag causes the orbital decay of planetesimals between the encounters — they migrate towards the Sun. This drift moves planetesimals which are located inside of the embryo’s orbit even further from it, facilitating the gap opening. On the other hand, on the outer side of the embryo’s orbit gas drag causes planetesimals to drift *towards* the embryo, and this tends to oppose the gap formation. As long as planetesimals are less massive than the embryo they are repelled by scattering in the same way independent of their mass. Thus, the question of whether the gap is cleared or not outside of embryo’s orbit depends only on the drag damping timescale; there exists a critical size r_{mig} such that planetesimals of this size, initially within $h \sim R_H$ of the embryo, after being repelled by roughly R_H , can migrate back the same distance in a synodic period. Only these planetesimals would be accreted by an isolated embryo: planetesimals with $r_p \gtrsim r_{mig}$ are too big to be brought back to the embryo by the gas drag and form a gap preventing their accretion. Planetesimals smaller than r_{mig} migrate so fast that in a synodic period they cross the embryo’s orbit and are lost to the inner disk. Embryo’s accretion would then be rather inefficient as well.

These problems arise only when an *isolated* protoplanetary core is considered. However, during the intermediate stages of planet formation it is almost certain that as a consequence of oligarchic growth (Kokubo & Ida 1998) there would be *many* embryos present in a disk at the same time. Their orbits should not be very widely separated: even if it were the case initially, subsequent increase in the embryo masses caused by the accretion of planetesimals would make these separations not very large in terms of their Hill radii (because R_H expands as embryo’s mass increases) and this is what is important for the dynamics.

When such a “crowded” population of protoplanetary cores (which is a natural outcome of the oligarchic growth) is present in the disk, gap formation is no longer an issue: although a particular embryo repels planetesimals by $\sim R_H$ and opens a gap in a single encounter, scattering by another embryo within $\sim t_{syn}$ pushes planetesimals back and spatially homogenizes the disk before they approach the first embryo again. Gap formation is thus suppressed and accretion can proceed almost un-

inhibited. On the other side of the problem, although the small shear-dominated planetesimals would still migrate through the orbit of some particular embryo, there would be many other embryos in the inner disk, meaning that these planetesimals will still be accreted in the end (although by some other embryo).

At a glance, it seems improbable that embryos can remain on purely circular and uninclined orbits in such configuration because at a radial separation of $\sim R_H$ they would strongly scatter each other and high random velocities would be quickly excited within a single synodic period. However, it turns out that there is a damping process in this problem — the dynamical friction by planetesimals — which can keep the embryo eccentricities low. For this to be the case the dynamical friction timescale t_{df} must be shorter than the time between encounters with the embryo, which is roughly t_{syn}/N if there are $N \sim 1$ protoplanetary cores per disk annulus of width R_H . Then the situation is similar to the scattering of shear-dominated planetesimals in the presence of the gas drag (see §3.1–3.4): random velocities are strongly excited during close approaches of embryos, but they are rapidly damped before next encounter occurs. As a result, embryos remain most of the time on uninclined⁴ and roughly circular orbits (i.e. their gravitational interaction is in the shear-dominated regime), and spacing of their semimajor axes can be as small as $\sim R_H$. They would occasionally collide with each other, growing in mass as a result, which would keep their orbital separations from becoming too small and maintain $N \sim 1$, but this does not affect the overall picture. We now estimate when such dynamically cold population of protoplanetary cores is possible.

The dynamical friction timescale can be estimated using the following formula (Stewart & Ida 2000):

$$t_{df} \approx \Omega^{-1} \frac{M_\odot}{M_e} \frac{M_\odot}{\Sigma_p a^2} \left(\frac{v}{\Omega a} \right)^4 \\ = \Omega^{-1} \left(\frac{M_e}{M_\odot} \right)^{1/3} \frac{M_\odot}{\Sigma_p a^2} \left(\frac{v}{\Omega R_H} \right)^4 \quad (50)$$

if the planetesimals responsible for friction are in the dispersion-dominated regime, i.e. $v \gtrsim \Omega R_H$ (we are dropping here all constant factors and the Coulomb logarithm). Then the critical mass $M_{e,crit}$ below which embryos are kept on kinematically cold orbits by the dynamical friction can be estimated from $t_{df} \approx t_{syn}/N$ to be

$$M_{e,crit} \equiv M_\odot \left(\frac{\Sigma_p a^2}{M_\odot} \right)^{3/2} \left(\frac{\Omega R_H}{v} \right)^6 N^{-3/2} \\ \approx 10^{25} g \left(\frac{\Omega R_H}{v} \right)^6 N^{-3/2} a_{AU}^{3/4}. \quad (51)$$

Note that the definition of $M_{e,crit}$ is similar to the definition of the isolation mass (e.g. Rafikov 2003b) although the dependence on v is very different. If most of the mass in solids is locked up in planetesimals ~ 1 km in size we would expect $v \sim \Omega R_H$, which would yield critical mass $\approx 10^{25} g$ at 1 AU and $\approx 10^{26} g$ at 30 AU. Thus, until M_e

⁴ Analogous to the planetesimal case, the shear-dominated scattering of embryos by embryos is very inefficient in exciting their vertical velocities.

reaches $10^{25} - 10^{26}$ g embryos scatter both small planetesimals and other embryos in the shear-dominated regime, and the spatial distribution of planetesimals in the disk is roughly homogeneous. When M_e passes the threshold (51), planetesimals can no longer keep embryos on kinematically cold orbits by dynamical friction and embryos quickly scatter each other, exciting large eccentricities and inclinations and switching into the dispersion-dominated regime. In this work we are not following this last stage of planetesimal disk evolution.

4. LOWER LIMIT ON PLANETESIMAL VELOCITY.

We have demonstrated in §3.1 that in the shear-dominated case planetesimal random velocity decays after scattering by the embryo as a result of the gas drag. If the damping time t_d is much shorter than the time between the encounters t_{syn} , planetesimal velocity right before the next approach to the embryo would be essentially zero ($\propto \exp(-t_{syn}/t_d)$ to be more exact). As a result, any subdominant sources of stirring which would normally be negligible become important in maintaining random motions at a finite value. These effects then determine the floor below which planetesimal random velocity cannot drop. Here we identify two such effects — scattering by the distant embryos and the stirring by large dispersion-dominated planetesimals — which determine the minimum horizontal and vertical random velocities of planetesimals respectively. We consider these two processes separately.

As we demonstrated in §3.6 the proto-Solar nebula should contain a population of dynamically cold embryos separated by roughly R_H/N — we again parametrize the uncertainty in their separation by the number of embryos N per R_H in radius. The surface number density of embryos is about $N/(2\pi a R_H)$.

Distant embryos scatter a given planetesimal quite frequently because both the velocity of incoming embryos (which is determined by the shear in the disk) and the number of passing embryos (for a fixed surface number density of embryos) increase linearly with the radial separation h . As a result, although the scattering by the nearest embryos is discrete, $t_d \ll t_{syn}/N$, the scattering by the embryos more distant than some critical h_c can be considered as a continuous process, similar to our treatment of the dispersion-dominated regime. To determine this critical distance we notice that scattering switches from the discrete to continuous mode when the average time between the passages of the embryos separated from planetesimal by less than h_c becomes shorter than the typical timescale on which planetesimal velocity would evolve otherwise. For planetesimals with $r_p \gtrsim r_{stop}$ this typical timescale is the gas damping timescale⁵ t_d .

The rate $\Gamma(h_c)$ at which embryos with $|h| < h_c$ pass a

particular planetesimal due to the shear in the disk is

$$\Gamma(h_c) = \frac{3\Omega}{2} \frac{N}{2\pi a R_H} \int_{-h_c}^{h_c} |h| dh = \Omega \frac{3}{4\pi} \frac{N}{a R_H} h_c^2. \quad (52)$$

Boundary between the discrete and continuous scattering is given by $\Gamma(h_c)t_d \approx 1$, meaning that

$$h_c \approx \left[\frac{4\pi}{3} \frac{a R_H}{N} (\Omega t_d)^{-1} \right]^{1/2} = R_H \left(\frac{4\pi}{3N} \frac{t_{syn}}{t_d} \right)^{1/2}. \quad (53)$$

Thus, $h_c \gg R_H$ for $N \sim 1$ and $t_d \ll t_{syn}$.

Since scattering by the embryos more distant than h_c occurs frequently on the gas damping timescale, the random component of scattering by these embryos averages to zero and we need to use equation (22) to evaluate the stirring by them. We find that

$$\begin{aligned} \frac{de^2}{dt} &= \frac{3\Omega}{2} \frac{N}{2\pi a R_H} \times 2 \int_0^{h_c} \langle \Delta(e^2) \rangle |h| dh \\ &\approx 5 \frac{3N}{4\pi} \Omega N \left(\frac{R_H}{a} \right)^3 \left(\frac{R_H}{h_c} \right)^2. \end{aligned} \quad (54)$$

Balancing this stirring by the gas damping $de^2/dt = -e^2/t_d$ and using (53) we find that the equilibrium value of eccentricity is

$$e_{min} \approx \sqrt{5} \frac{3N}{4\pi} \frac{R_H}{a} \frac{t_d}{t_{syn}}. \quad (55)$$

Random velocity is below the Hill velocity whenever $t_d \lesssim t_{syn}/N$. Using (10)-(12) we evaluate

$$e_{min} \approx 0.04 N \frac{R_H}{a} \left(\frac{M_e}{10^{25} \text{ g}} \right)^{1/3} \frac{r_p}{10 \text{ m}} a_{AU}^{5/4}, \quad (56)$$

$$e_{min} \approx 0.03 N \frac{R_H}{a} \left(\frac{M_e}{10^{25} \text{ g}} \right)^{1/3} \left(\frac{r_p}{10 \text{ m}} \right)^2 \left(\frac{a_{AU}}{5} \right)^{-5/4} \quad (57)$$

$$e_{min} \approx 0.05 N \frac{R_H}{a} \left(\frac{M_e}{10^{25} \text{ g}} \right)^{1/3} \frac{r_p}{10 \text{ m}} \left(\frac{a_{AU}}{30} \right)^{3/2}, \quad (58)$$

for quadratic, Stokes, and Epstein drag regimes respectively. These estimates imply that the minimum horizontal random velocities of small planetesimals are below the Hill velocity, as it should be. For 10 m planetesimals in the vicinity of 10^{25} g embryo e_{min} corresponds to velocities of the order of 1 m s^{-1} in the inner part of the proto-Solar nebula, dropping to $\approx 0.5 \text{ m s}^{-1}$ at 30 AU (mainly because the orbital velocity scales as $a^{-1/2}$).

Scattering by the distant embryos cannot however maintain the inclinations of small planetesimals at a finite level. The excitation of the vertical velocity by an encounter with the embryo separated even by R_H from planetesimal is weakened compared to the excitation of horizontal velocity by the geometric factor $ia/R_H \ll 1$. As a result, the growth rate of inclination due to the embryo scattering scales as i^2 (exactly like gas drag) and for $t_d \lesssim t_{syn}$ gas drag unconditionally dominates. We now consider if the stirring by the rest of planetesimal population can keep inclinations of small bodies finite.

Gas drag acting on large planetesimals (bigger than 0.1–1 km depending on the location in the nebula, see

⁵ Note that for planetesimals smaller than r_{stop} gas damping time is shorter than Ω^{-1} . However the duration of the gravitational interaction with the distant embryo is always $\sim \Omega^{-1}$ meaning that typical velocity evolution timescale for planetesimals with $r_p \lesssim r_{stop}$ is not t_d but rather Ω^{-1} . This, however, is only important for very small planetesimals, $r_p \lesssim 1 \text{ m}$ (see Figure 1), which are not covered by this study anyway.

§3.5) is too weak to prevent them from staying in the dispersion-dominated regime with respect to the embryo. Their gravitational interaction with small planetesimals is certain to take place in the dynamically “hot” regime (because for the same physical velocity the Hill radius for the planetesimal-planetesimal scattering is much smaller than R_H for the embryo-planetesimal scattering).

Rafikov (2003c) has demonstrated that the velocity excitation by planetesimals sensitively depends on the planetesimal mass spectrum. For a given differential surface number density distribution of planetesimals dN/dm the velocity stirring can be written as (Rafikov 2003c)

$$\frac{dv^2}{dt} \approx \Omega(\Omega a)^2 \left(\frac{\Omega a}{V}\right)^2 \frac{a^2}{M_\odot^2} \int \frac{dN(m)}{dm} m^2 dm, \quad (59)$$

where V is the random velocity of the dispersion-dominated planetesimals (which we set constant for simplicity). Because of the stirring by the embryos this velocity should be some multiple of ΩR_H , but owing to the action of the gas drag (and maybe also planetesimal dynamical friction) it is not higher than several ΩR_H , see equations (27), (42), and (46).

Numerical simulations very often produce planetesimal mass spectra such that $dN/dm \propto m^{-\alpha}$ with $\alpha \approx 2.5$ within some wide range of masses (Kokubo & Ida 1996). In a disk with such spectrum most of the mass is concentrated in the lower end of the distribution while the most of the stirring is done by its upper end (Rafikov 2003c). We will assume that the planetesimal mass spectrum has such a power-law form for $m_0 \lesssim m_p \lesssim m_*$, where we take somewhat arbitrarily $m_0 = 10^{16}$ g and $m_* \approx 10^{22}$ g (roughly 1-km and 100-km size planetesimals). The inclination excitation by the largest planetesimals ($m_p \approx m_*$, which are still much smaller than the embryos!) can be roughly expressed in terms of these masses and planetesimal surface mass density Σ_p (dominated by bodies with $m_p \approx m_0$) as

$$\frac{di^2}{dt} \approx \Omega \left(\frac{\Omega a}{V}\right)^2 \frac{m_0 \Sigma_p a^2}{M_\odot^2} \left(\frac{m_*}{m_0}\right)^{3-\alpha}. \quad (60)$$

In writing down this expression we have assumed that large planetesimals are numerous enough to give rise to a continuous rather than discrete stirring. Balancing (60) with $-i^2/t_d$ we find the equilibrium value of inclination:

$$i_{min} \approx \frac{\Omega a}{V} \left[\Omega t_d \frac{m_0 \Sigma_p a^2}{M_\odot^2} \left(\frac{m_*}{m_0}\right)^{3-\alpha} \right]^{1/2}. \quad (61)$$

Evaluating this expression for $V = 3\Omega R_H$, $M_e = 10^{25}$ g, Σ_p given by (2), t_d given by (10)-(12), and our adopted values of m_0 , m_* , and $\alpha = 2.5$ we find that

$$i_{min} \approx 10^{-4} \frac{R_H}{a} \left(\frac{r_p}{10 \text{ m}}\right)^{1/2} a_{7/8}^{7/8}, \quad (62)$$

$$i_{min} \approx 10^{-4} \frac{R_H}{a} \frac{r_p}{10 \text{ m}} \left(\frac{a_{AU}}{5}\right)^{-3/8}, \quad (63)$$

$$i_{min} \approx 3 \times 10^{-4} \frac{R_H}{a} \left(\frac{r_p}{10 \text{ m}}\right)^{1/2} \frac{a_{AU}}{30}, \quad (64)$$

for corresponding drag regimes. These values of inclination correspond to very small vertical velocities of planetesimals, of the order of a 1 cm s⁻¹ in the vicinity of

10²⁵ g protoplanetary core. Evidently, this type of stirring would not be able to affect minimum planetesimals eccentricities, since $i_{min} \ll e_{min}$, see (56)-(58).

Scattering by large planetesimals would perturb embryo orbits as well. Balancing the stirring rate (61) with the dynamical friction rate (using timescale t_{df} , see [50]), we find that the minimum inclination of the embryo $i_{e,min}$ is about

$$i_{e,min} \approx \frac{R_H}{a} \left(\frac{\Omega R_H}{V}\right) \left(\frac{v}{\Omega R_H}\right)^2 \left[\frac{m_0}{M_e} \left(\frac{m_*}{m_0}\right)^{3-\alpha} \right]^{1/2} \\ \approx 10^{-3} \frac{R_H}{a} \left(\frac{\Omega R_H}{V}\right) \left(\frac{v}{\Omega R_H}\right)^2 \left(\frac{M_e}{10^{25} \text{ g}}\right)^{-1/2}, \quad (65)$$

provided that the time between encounters with large planetesimals (which dominate stirring) is shorter than t_{df} (for continuous approximation to hold). As a bottom line, scattering by large planetesimals would keep inclinations of small bodies relative to protoplanetary cores at the level of $\sim 10^{-3}(R_H/a)$, most likely via the stirring of the cores.

There are other possibilities for maintaining inclinations of shear-dominated planetesimals at some minimum level. One of them is the gravitational scattering between small planetesimals themselves which transfers the energy of random motion from horizontal into the vertical direction. This is likely not to be important because the dynamical relaxation of small bodies moving at random velocities $\gtrsim e_{min}\Omega a$ is very slow. Another process is the gravitational instability in the thin layer (P.Goldreich, private communication) which may excite random velocities of small constituent bodies. Instability would operate if the planetesimal velocity dispersion is below $\chi\pi G\Sigma_p/\Omega \approx 30 \text{ cm s}^{-1} \chi$ (usual Toomre criterion), and this is below $e_{min}\Omega a$ even for $\chi = 1$. Finally, inelastic collisions between small planetesimals can heat the disk vertically, and we elaborate more on this in the next section.

5. INELASTIC COLLISIONS.

Inelastic collisions between planetesimals can effectively damp their random velocities. The escape speed from the surface of the 100 m planetesimal is about 10 cm s⁻¹ and planetesimals are typically moving with higher velocities (see [56]-[58]), which means that (a) they would lose a lot of energy in high-energy collisions, and (b) gravitational focusing is unimportant and collision cross-section is almost equal to the geometric cross-section. Assuming that planetesimals lose a fraction ~ 1 of their energy when they collide, we estimate the velocity damping by inelastic collisions to be

$$\frac{dv^2}{dt} \approx -\Omega v^2 \frac{\chi \Sigma_p}{\rho r_p} \frac{v_h}{v_z}, \quad (66)$$

where we again assumed that only a fraction χ of solid mass is in the shear-dominated planetesimals. From this expression it is clear that inelastic collisions lead to the exponential damping of velocity (if $v_h/v_z \approx \text{const}$) on a timescale

$$t_{inel} \equiv \Omega^{-1} \chi^{-1} (\rho_p r_p / \Sigma_p) (v_z / v_h). \quad (67)$$

The importance of inelastic collisions is judged by comparing t_{inel} with t_d — damping time due to the gas drag.

Using equations (10)-(12) we find

$$t_d/t_{inel} \approx 0.25 \chi (v_h/v_z) a_{AU}^{-1/4}, \quad (68)$$

$$t_d/t_{inel} \approx 0.1 \chi (v_h/v_z) \left(\frac{r_p/\lambda}{10} \right), \quad (69)$$

$$t_d/t_{inel} \approx 0.01 \chi (v_h/v_z), \quad (70)$$

for quadratic, Stokes, and Epstein gas drag regimes correspondingly. These estimates clearly demonstrate that $t_d \lesssim t_{inel}$ whenever $v_z \sim v_h$ ($i \sim e$), meaning that inelastic collisions are unimportant when planetesimal velocities are roughly isotropic. This is always true in the dispersion-dominated regime allowing us to neglect inelastic collisions in this case.

The situation is different in the shear-dominated regime where one can easily have $v_z \ll v_h$. Let's assume that planetesimal inclination right before the encounter with the embryo is very low. Right after the encounter inclination remains roughly the same (see [24]) while the eccentricity increases to $\sim (R_H/a) \gg i_{min}$; as a consequence, t_{inel} immediately becomes much shorter than t_d and inelastic collisions suddenly become more important than gas drag. However, this is a very transient stage because inelastic collisions not only dissipate energy but can also isotropize the velocities of colliding bodies. If planetesimals were colliding like rigid balls, bouncing off after collision, one would expect roughly isotropic recoil velocities. Consequently, one would obtain $v_z \approx v_h$ after every planetesimal has experienced a single physical collision, i.e. after time t_{inel} has passed since the scattering by the embryo. This immediately increases the efficiency of the gas drag and makes it more important for the random velocity dissipation shortly after scattering has occurred, see (68)-(70).

After that, according to (49), inclination decays with time slower than eccentricity does meaning that the role of inelastic collisions keeps decreasing. If the time interval between the successive encounters with the embryo is long enough, the eccentricity decay will stop at the asymptotic value e_{min} (of course, with occasional oscillations due to scattering by distant embryos) while the inclination would still decay further until it reaches $i_{min} \ll e_{min}$. On this stage v_z/v_h goes down and physical collisions can again start occurring quite frequently; however the imminent isotropization of velocities after every collision limits their importance (in comparison with gas drag) only to short periods of time. As a result, the timescale of velocity damping between encounters with embryos would still be very close to the gas damping time t_d .

Physical collisions might affect the determination of i_{min} since they can be effective at pumping the energy of horizontal motions into vertical ones. The minimum velocity anisotropy v_z/v_h they provide can be determined from the condition $t_d/t_{inel} \approx 1$ and turns out to be roughly 0.25χ , 0.1χ , and 0.01χ for typical parameters of quadratic, Stokes, and Epstein drag regimes, see equations (68)-(70). At the same time, in corresponding cases the dispersion-dominated scattering by large planetesimals gives rise to $v_z/v_h \approx 3 \times 10^{-3}$, 3×10^{-3} , 6×10^{-3} (see [56]-[58] and [62]-[64]). Thus, we may conclude that for large values of χ ($\gtrsim 0.1$) inelastic collisions are important in setting the minimum value of planetesimal inclination for quadratic and Stokes drag regimes. This may

be the case in the inner proto-Solar nebula, inside 5 – 10 AU. Outside this region, where the Epstein drag acts on the shear-dominated planetesimals, inelastic collisions are important only for $\chi \approx 1$. However, the minimum *relative* inclination between small planetesimals and embryos would still be determined by the gravitational effect of large planetesimals (even in the inner Solar System, for $\chi \lesssim 0.1$), see (65).

This discussion has assumed rather idealized model of planetesimal collisions. In reality high-energy collisions are likely to be catastrophic, leading to the disruption of participant bodies. Then the amount of kinetic energy transferred into vertical motions and the degree of isotropization would be determined by the ejection velocity of the resulting debris. Velocity dispersions in collisional families of asteroids (Zappala et al. 1996) and results of numerical simulations (Michel et al. 2003) indicate that the ejection velocities are considerably smaller than the initial planetesimal velocities. This would slow down the velocity isotropization compared to the case of collisions of “hard balls”. Nevertheless, we do not expect this to seriously change the general picture outlined before. Besides, it is not at all clear by how much these velocities would differ in the case of the planetesimals (10-100 m in size, strength-dominated fragmentation) colliding at several tens of m s^{-1} , since the collisions between 10-km asteroids (gravity-dominated fragmentation) on which information exists occur at relative speeds of several km s^{-1} .

6. ACCRETION OF LOW-ENERGY PLANETESIMALS.

Protoplanetary embryos grow by accreting planetesimals. Accretion in differentially rotating disks is intrinsically complicated because of the three-body gravitational interaction of the two merging bodies and the central mass. One can however greatly simplify consideration by treating accretion as a two-body process while approximately taking into account three-body effects by limiting planetesimal approach velocity relative to the embryo by ΩR_H from below. This is a direct consequence of the shear present in the disk.

With this in mind we can write a rather general formula for the protoplanetary mass accretion rate:

$$\begin{aligned} \frac{dM_e}{dt} &\approx n_p m_p R_e^2 v_a \left(1 + \frac{v_{esc}^2}{v_a^2} \right) \\ &\approx \Omega \Sigma_p R_H^2 \frac{R_e}{R_H} \frac{v_a}{v_z} \left(\frac{\Omega R_H}{v_a} \right)^2, \end{aligned} \quad (71)$$

where R_e is the physical size of the embryo and the last equality holds for $v_a \ll v_{esc}$ — the most relevant for us case. The ratio R_e/R_H is independent of the embryo's mass but varies with the distance from the Sun:

$$R_e/R_H \equiv \left(\frac{3}{4\pi} \frac{M_\odot}{\rho_p a^3} \right)^{1/3} \approx 5.2 \times 10^{-3} a_{AU}^{-1}. \quad (72)$$

In the dispersion-dominated case the scattering of planetesimals by the embryo always tends to maintain $v_z \sim v \approx v_a \gtrsim \Omega R_H$, thus

$$\frac{dM_e}{dt} \approx \Omega \Sigma_p R_H^2 \frac{R_e}{R_H} \left(\frac{\Omega R_H}{v} \right)^2. \quad (73)$$

In the shear-dominated case approach velocity v_a is almost independent of planetesimal eccentricity or inclination and is solely determined by ΩR_H . At the same

time, the vertical velocity of planetesimals which sets the thickness of planetesimal disk is smaller than ΩR_H , and we find that

$$\frac{dM_e}{dt} \approx \Omega \Sigma_p R_H^2 \frac{R_e}{R_H} \frac{\Omega R_H}{v_z}. \quad (74)$$

The derivation of equation (71) has implicitly assumed that the maximum impact parameter at which planetesimal can be accreted by the embryo $R_e \sqrt{1 + v_{esc}^2/v_a^2}$ is smaller than the planetesimal disk thickness v_z/Ω . In the shear-dominated case, when $v_a \sim \Omega R_H \ll v_{esc}$, this sets a limit on the vertical velocity of planetesimals at which their accretion can be described by equation (71):

$$v_z \gtrsim v_{z,cr} \equiv \Omega R_H (R_e/R_H)^{1/2} \approx 0.07 \Omega R_H a_{AU}^{-1/2} \quad (75)$$

(Greenberg et al. 1991; Dones & Tremaine 1993). Thus, equation (74) is applicable only for $v_z \gtrsim v_{z,cr}$. Whenever $v_z \lesssim v_{z,cr}$ planetesimal disk is geometrically very thin and embryo can accrete the whole vertical column of material it encounters (eccentricity is only restricted to be smaller than R_H/a). In this case one can easily show that

$$\begin{aligned} \frac{dM_e}{dt} &\approx \Omega \Sigma_p R_e R_H \left(1 + \frac{v_{esc}^2}{v_a^2}\right)^{1/2} \\ &\approx \Omega \Sigma_p R_H^2 \left(\frac{R_e}{R_H}\right)^{1/2}. \end{aligned} \quad (76)$$

This is the highest possible accretion rate of planetesimals by the embryo that can be achieved for various dynamical states of the planetesimal disk.

It is plausible that most of the planetesimal mass is concentrated in the bodies with sizes of about 1–10 km which interact with the embryo in the dispersion-dominated regime. According to (73) the growth timescale of the embryo is then

$$\begin{aligned} t_{g,dd} &\approx \Omega^{-1} \left(\frac{M_e}{M_\odot}\right)^{1/3} \frac{M_\odot}{\Sigma_p a^2} \frac{R_H}{R_e} \left(\frac{v}{\Omega R_H}\right)^2 \\ &\approx 10^5 \Omega^{-1} \left(\frac{M_e}{10^{25} \text{g}}\right)^{1/3} \left(\frac{v}{\Omega R_H}\right)^2 a_{AU}^{1/2}. \end{aligned} \quad (77)$$

Using equations (27), (42), and (46) we find that the time needed to build 10^{25} g protoplanetary core by the accretion of such dispersion-dominated planetesimals is $\approx 10^5$ yr at 1 AU, $\approx 4 \times 10^6$ yr at 5 AU, and $\approx 3 \times 10^7$ yr at 30 AU.

At the same time, a fraction $\chi < 1$ of planetesimal mass can be in small bodies which are shear-dominated with respect to the embryo. This mass is concentrated in a vertically thin population and comparing (62)-(64) & (65) with (75) we see that the vertical velocity of planetesimals in the subdisk is smaller than $v_{z,cr}$. Thus, the shear-dominated planetesimals are absorbed very efficiently by the embryo, and we find using (76) that the embryo's growth timescale due to their accretion is

$$\begin{aligned} t_{g,sd} &\approx \chi^{-1} \Omega^{-1} \left(\frac{M_e}{M_\odot}\right)^{1/3} \frac{M_\odot}{\Sigma_p a^2} \left(\frac{R_H}{R_e}\right)^{1/2} \\ &\approx 7 \times 10^3 \chi^{-1} \Omega^{-1} \left(\frac{M_e}{10^{25} \text{g}}\right)^{1/3}. \end{aligned} \quad (78)$$

This is $\approx 10^3 \chi^{-1}$ yr at 1 AU, $\approx 10^4 \chi^{-1}$ yr at 5 AU, and $\approx 2 \times 10^5 \chi^{-1}$ yr at 30 AU. Thus, even if only about 1% of the mass in solids is locked up in the barely inclined shear-dominated planetesimals ($\chi = 10^{-2}$) they would dominate the accretion rate of the embryo because $t_{g,sd} \lesssim t_{g,dd}$!

7. DISCUSSION.

The outlined picture of planetesimal dynamics in the gaseous nebula naturally divides planetesimals of different sizes into two well-defined populations with respect to the scattering by a set of protoplanetary embryos. One is a “hot” population of bodies bigger than 0.1–1 km which gravitationally interact with embryos in the dispersion-dominated regime and have large enough inclinations for the scattering to be an intrinsically three-dimensional process. The other is a “cold” populations of smaller planetesimals (sizes below 0.1-1 km) which interact with embryos in the shear-dominated regime. These planetesimals tend to be confined to a vertically thin disk [with a thickness of $\lesssim 10^{-3} R_H$] near the nebular midplane by the action of the gas drag.

The difference between these populations is most striking when the accretion of planetesimals by the embryos is concerned. Accretion of hot planetesimals allows 10^{25} g embryo to double its mass in $\sim 10^5$ yr in the terrestrial planet region and in several 10^7 yr in the region of ice giants. The latter timescale is quite long from the cosmogonical point of view. At the same time, the accretion of cold planetesimals is about 100 times faster, with mass doubling timescale of $\sim 10^3$ yr and $\sim 10^5$ yr in the inner and outer parts of the nebula, provided that *all* solid mass is locked in these small planetesimals. Formation of gaseous atmospheres around massive protoplanetary cores accelerates absorption of small bodies even more: gaseous envelopes can be very efficient at trapping small planetesimals (Inaba & Ikoma 2003), thus increasing the capture radius R_e by a factor of several and shortening the growth timescale, see equation (78). Protoplanetary cores would also grow by merging with other cores (since they reside on closely spaced orbits, see §3.3.6) and this process is regulated by the degree of overlap of their Hill spheres; apparently, the faster the cores grow, the closer their orbits are in the Hill coordinates, and the faster they merge.

It is possible that in the proto-Solar nebula most of the mass was concentrated not in the dynamically cold population of small planetesimals but rather in 1-10 km bodies belonging to the hot population. In this case, although there is a huge reservoir of solid mass potentially available for the accretion, embryo can hardly make use of it because hot planetesimals are accreted rather inefficiently, see equation (77). At the same time, the cold population which can potentially allow a vigorous growth of the embryo might simply not contain enough surface density to ensure high enough accretion rate (accretion timescale is inversely proportional to the fraction of mass contained in small planetesimals, see [78]). Thus, unless enough mass can be transferred from hot to cold planetesimals, embryos would be stuck in a rather slow growth mode.

Fragmentation is a natural process for channeling the mass from the big bodies into small ones and it should be taking place near massive embryos. Indeed, the es-

cape speed from the surface of 1 km body is about 1 m s^{-1} , while the Hill velocity of 10^{25} g embryo is $\approx 50 \text{ m s}^{-1}$ at 1 AU and is $\approx 10 \text{ m s}^{-1}$ at 30 AU. Thus, planetesimals containing most of the solid mass in the disk would collide with kinetic energy exceeding their gravitational binding energy. Depending on the internal strength of planetesimals, such collisions can lead to the disruption of parent bodies into a number of smaller fragments. Collision strength is likely to be very small for bodies in the outer Solar System which are thought to be primarily composed of ices. Comets are presumably the closest existing analogs of planetesimals which formed far from the Sun and they are known to have small internal strength, e.g. from the observations of the disruption of Shoemaker-Levy comet by the tidal field of Jupiter (Greenberg et al. 1995). Thus, it would be natural to expect that the collisional fragmentation triggered by the dynamical excitation of planetesimals by massive protoplanetary cores would readily occur at least in the outer Solar System.

Efficiency of fragmentation depends on a collision timescale t_{inel} of planetesimals containing most of the solid mass. For 1 km bodies using (67) we estimate it to be $\sim 10^3 \text{ yr}$ at 1 AU and $\gtrsim 10^7 \text{ yr}$ at 30 AU. In the outer Solar System this might seem like a rather long timescale but one should keep in mind that channeling just 10% of mass into the population of cold planetesimals would increase the embryo's accretion rate by a factor of ≈ 10 compared to the accretion of dispersion-dominated bodies, and this can be accomplished in a time 10 times shorter than t_{inel} , i.e. in about several Myr. Note that according to (78) the characteristic growth time of 10^{25} g embryo by accretion of small bodies (for $\chi \approx 0.1$) is also several Myr. Growth time decreases when χ goes up meaning that several Myr is a natural mass evolution timescale for such embryos in the outer Solar System. If accretion of small planetesimals turns out to be the dominant mode of the embryo's growth, the planet formation timescale might be intimately related to the timescale of fragmentation of massive planetesimals in catastrophic collisions.

The behavior of the embryo's accretion rate would in the end depend on the details of the time evolution of the mass fraction in small planetesimals χ . Scaling of χ with time would also determine whether inelastic collisions between small planetesimals are an important dynamical factor; as we demonstrated in §5, this can in some cases be an issue in the inner parts of the protoplanetary nebula. The amount of solid material contained in small planetesimals is determined by (1) the input of mass due to the fragmentation of large planetesimals, (2) the removal of mass via the accretion by embryos, and (3) the evolution of the surface density of small planetesimals due to the random scattering by embryos and their gas drag induced inward migration (Weidenschilling 1977; Thommes et al. 2003). A self-consistent calculation of χ has to combine all these contributions and is beyond the scope of this study.

Rapid accretion of small planetesimal can proceed provided that not only small bodies but also embryos themselves are on almost circular and uninclined orbits. As we demonstrated in §3.3.6, if oligarchic growth allows the existence of many protoplanetary cores in the nebula, this is only possible for the cores lighter than about

$10^{25} - 10^{26} \text{ g}$, when dynamical friction by planetesimals can keep embryo's random motions small. It is not clear what happens beyond this mass but most likely embryos would be dynamically excited ($e, i \gtrsim R_H/a$) and even if small planetesimals can still be kept confined to a cold, thin disk, embryo's accretion would proceed in a less efficient dispersion-dominated regime (because relative embryo-planetesimal velocity is increased above ΩR_H). Thus, the acceleration of embryo's growth by the accretion of small planetesimals would likely work only for small enough embryos (less massive than the Moon or Mars).

The discrete nature of the shear-dominated scattering of small planetesimals by the embryos is very important for accurate calculation of processes such as the disruption of small planetesimals in catastrophic collisions or any other process characterized by the energy threshold. Usual continuous approximation suitable in the dispersion-dominated case would not work for such processes because it characterizes planetesimal velocity by its average value which is either above or below the threshold, meaning that corresponding process is either always on or always off. In reality, planetesimal velocity changes continuously between the encounters with embryos from very large values (about ΩR_H) to very small ones. As a result, planetesimal velocity can be above the threshold for some time and during this period corresponding process would operate. Later on velocity would drop below the threshold and process would switch off. This is qualitatively different from what one would obtain using the continuous description for the planetesimal scattering in the shear-dominated regime. For the fragmentation of small bodies this implies that planetesimal destruction in catastrophic collisions proceeds in bursts right after each passage of the embryo, when relative planetesimal velocities are high, but later on when velocities are damped by the gas drag, collisions might not be energetic enough to continue fragmenting planetesimals.

8. CONCLUSIONS.

We have explored the details of planetesimal dynamics in the vicinity of protoplanetary embryo in the presence of gas. Our study has concentrated on small planetesimals (out of the whole planetesimal size distribution), $\lesssim 10 \text{ km}$ in size, which can be strongly affected by the gas drag. We showed that largest of them, $\gtrsim 1 \text{ km}$, are kept in the dispersion-dominated regime by the embryo's scattering, although their average velocities are reduced by the gas drag. Planetesimals smaller than roughly $0.1 - 1 \text{ km}$ (depending on the location in the nebula) interact with protoplanetary embryos in the shear-dominated regime. Owing to the action of the gas drag these planetesimals settle into a vertically thin layer near the nebular midplane; they also experience very strong velocity damping between consecutive encounters with the embryos which allows them to approach embryos every time with the relative velocity comparable to the Hill velocity — minimum velocity which can be achieved in a differentially rotating disk.

For different locations in the proto-Solar nebula we have determined which planetesimals are only weakly affected by the gas drag and are in the dispersion-dominated regime, and which planetesimals are so strongly coupled to the gas that their velocities are below

the Hill velocity of the protoplanetary cores. Dynamical peculiarities of the shear-dominated regime in the presence of gas lead to a very high efficiency of accretion of small planetesimals by the embryos. If the surface mass density of small bodies is high enough ($\gtrsim 1\%$ of the total surface density in solids) their accretion would dominate the embryo's growth (relative to the accretion of bigger, dispersion-dominated planetesimals).

Larger planetesimals, $\gtrsim 1$ km in size, likely containing most of the mass in solids, are excited by the gravity of the embryos and are not very efficiently accreted by them. They will collide with each other at high velocities and fragment into smaller pieces contributing to the population of small planetesimals. Thus, the embryo's growth via the accretion of small shear-dominated planetesimals can be regulated by the fragmentation of bigger, dispersion-dominated bodies. Planetesimal fragmentation would probably be the easiest in the outer Solar System where the colliding bodies are mostly composed of ices and are therefore internally weak and susceptible to easy destruction. The natural timescale for the growth of the 10^{26} g protoplanetary embryo at 30 AU from the Sun by the accretion of small planetesimals turns out to be around several Myr. This scenario would

work only if a population of protoplanetary cores formed as the outcome of oligarchic growth can be kept on almost non-inclined and circular orbits. As we demonstrated in §3.3.6, this is possible if the embryo mass does not exceed $10^{25} - 10^{26}$ g (depending on the distance from the Sun), since in this case the dynamical friction by planetesimals can successfully counteract embryo's stirring.

Future work should address the issues of the self-consistent evolution of the mass fraction χ locked up in the small planetesimals; the role of the inelastic collisions using improved fragmentation physics (can be an issue in the inner Solar System); the final fate of the embryos more massive than $\approx 10^{26}$ g which cannot be kept dynamically cold by the planetesimal dynamical friction, and so on.

I am grateful to Jeremy Goodman for always stressing to me the importance of gas for the planetesimal dynamics. I have greatly benefited from numerous discussions with Peter Goldreich who has been working on similar problems. Author is a Frank and Peggy Taplin Member at the IAS; he is also supported by the W. M. Keck Foundation and NSF grant PHY-0070928.

REFERENCES

- Adachi, I., Hayashi, C., & Nakazawa, K. 1976, *Prog. Theor. Phys.*, 56, 1756
 Dones, L. & Tremaine, S. 1993, *Icarus*, 103, 67
 Greenberg, R., Bottke, W. F., Carusi, A., & Valsecchi, G. B. 1991, *Icarus*, 94, 98
 Greenberg, J. M., Muzitani, H., & Yamamoto, T. 1995, *A&A*, 295, L35
 Hasegawa, M. & Nakazawa, K. 1990, *A&A*, 227, 619
 Hénon, M. & Petit, J. M. 1986, *Celest. Mech.*, 38, 67
 Ida, S. & Makino, J. 1993, *Icarus*, 106, 210
 Inaba, S. & Ikoma, M. 2003, *A&A*, 410, 711
 Kokubo, E. & Ida, S. 1996, *Icarus*, 123, 180
 Kokubo, E. & Ida, S. 1998, *Icarus*, 131, 171
 Landau, L. D. & Lifshitz, E. M., *Fluid Mechanics*; Pergamon Press, 1987
 Michel, P., Benz, W., & Richardson, D. C. 2003, *Nature*, 421, 608
 Rafikov, R. R. 2001, *AJ*, 122, 2713
 Rafikov, R. R. 2003a, *AJ*, 125, 922
 Rafikov, R. R. 2003b, *AJ*, 125, 942
 Rafikov, R. R. 2003c, *AJ*, 126, 2529
 Safronov, V. S. 1969, *Evolution of the Protoplanetary Cloud and Formation of the Earth and Planets* (Nauka, Moscow, 1969)
 Stewart, G. R. & Ida, S. 2000, *Icarus*, 143, 28
 Thommes, E. W., Duncan, M. J., & Levison, H. F. 2003, *Icarus*, 161, 431
 Wetherill, G. W. & Stewart, G. R. 1989, *Icarus*, 74, 542
 Weidenschilling, S. J. 1977, *MNRAS*, 180, 57
 Whipple, S. J. 1977, *MNRAS*, 180, 57
 Zappala, V., Cellino, A., Dell'oro, A., Migliorini, F., & Paolicchi, P. 1996, *Icarus*, 196, 124, 156